www.elsevier.com/locate/ijadhadh

The Mixed-Mode Fracture Behaviour of Epoxy By The Compact Tension Shear Test

J. Jamali, Y. Fan, J.T. Wood

PII: S0143-7496(15)00122-0
DOI: http://dx.doi.org/10.1016/j.ijadhadh.2015.08.006
Reference: JAAD1696

To appear in: *International Journal of Adhesion and Adhesives*

Received date: 27 October 2014
Accepted date: 8 August 2015

Cite this article as: J. Jamali, Y. Fan and J.T. Wood, The Mixed-Mode Fracture Behaviour of Epoxy By The Compact Tension Shear Test, *International Journal of Adhesion and Adhesives,* http://dx.doi.org/10.1016/j.ijadhadh.2015.08.006

THE MIXED-MODE FRACTURE BEHAVIOUR OF EPOXY BY THE COMPACT TENSION SHEAR TEST

J. Jamali*, Y. Fan, and J.T. Wood

Mechanical and Materials Engineering Department, University of Western Ontario, London, Canada

* Corresponding author (jjamali@alumni.uwo.ca)

Keywords: *Mixed mode fracture, Failure model, Epoxy, CTS specimen*

Abstract

In this study, pure mode I, pure mode II and mixed mode fracture behaviour of an epoxy were investigated. Specifically, the mixed mode values of fracture toughness and critical strain energy release rate (CSERR) were measured. Specimens were subjected to mixed mode loading using compact tension shear (CTS) test. Some experimental modifications were found to be necessary to eliminate rotation and ensure crack propagation at the notch when testing epoxy specimens at high mode II loading. A failure criterion for the mixed mode loading of polymer is developed and its predictions are compared with the experimental results. The crack propagation direction in epoxy was investigated in this research as well. A detailed study of failure mechanisms on the fracture surface was performed. The results indicate that the increase in the value of toughness can be directly related to the fracture morphology.

1. Introduction

The prediction of the fracture behaviour of polymer composite materials is a complex undertaking that has necessarily involved at least some degree of empiricism [1–4]. With the long-term goal of being able to design composite systems for optimized energy absorption, it would be highly beneficial to develop a predictive fracture model that is based solely on the properties of the constituent phases, the interface between them and the geometric details of the microstructure. Owing to the high degree of constraint resulting from closely packed fibre reinforcement, the matrix of a polymer composite shares similarities with adhesive joints, in this paper, we begin with the characterization of a common epoxy

system subjected to mode I, mode II and mixed mode I/II loading as a first step on the path to a predictive model for the mixed mode fracture polymer composite systems. To obtain such a model it is required to study the fracture behavior of bulk polymer and to relate the amount of energy released in the fracture of a confined polymer in a polymer composite or a bonded joint. The full investigation of polymer fracture is carried out in this research.

2. Background

The study of mode I toughness in polymers and polymer joints has been performed by several researchers using bend test or compact tension specimen [5–8]. However, the mixed mode fracture toughness of neat polymer has been studied by few researchers. Maccagno and Knott [9] studied the mixed mode behaviour of PMMA using four-point bending test of a beam and they compared their results with three fracture criteria. They concluded that a maximum tensile stress criterion well-described the material behaviour. Chen etal [10] used J-integral contour to compute mixed mode strain energy release rate in polymer bonds. Araki et al. [11] investigated the mixed mode crack angle of an epoxy and compared it with the existing criteria. They also studied the effect of the glass transition temperature on the toughness. The measurement of mixed mode fracture response of epoxy was carried out using beam specimens subjected to three-point or four-point bending tests. Apart from reporting the values of toughness and comparing them with empirical failure criteria, the contribution of the fracture mechanisms to the value of toughness was not studied by these researchers. Bruce [12] compared the fracture surface of polymer specimens subjected to pure mode I and pure mode II loading and found the mode II CSERR to be 2.4 times greater than the mode I value. Observations of the respective fracture surfaces revealed that the mode II surface consisted of 45 degree hackles compared to the flat surface of the mode I specimens and led to the conclusion that in increased mode II CSERR is due to solely the increased crack path length, $L = L_0\left(1 + \sqrt{2}\right)$, resulting from hackle formation.

To study mixed mode loading, the beam methods require different types of specimens or testing for different modes of loading. However, the CTS test described by Richard [13] requires only one specimen geometry for the whole range of mixed mode loading.

3. Experimental Method

3.1 Materials and Manufacturing

The neat epoxy specimen in this study was made using CLR1180/CLH6560 epoxy material from Crosslink Tech. Inc. The epoxy was made by mixing hardener and resin in a ratio recommended by the manufacturer (100 units of resin to 30 units of the hardener). In mixing the resin and the hardener, particular care was taken to avoid introducing air bubbles into the mixture. After mixing, the resin was poured into trays or molds that were lined with Teflon vacuum bags to avoid resin adhering to the trays. The curing process took 48 hours at room temperature. Cured specimens were then cut to the test dimension by a milling machine (see Fig. 1).

3.2 Tensile Testing

Tensile testing of epoxy specimens was carried out according to standard ASTM D638 [14]. Totally 6 dumbbell shape specimens with gage length of 50 mm were tested at strain rates between $6.7 \times 10^{-4}\ \frac{1}{s}$ and $1.7 \times 10^{-3}\frac{1}{s}$. To measure the gage displacement and strain precisely a 50 mm gage length extensometer was used. The average values of different mechanical properties of epoxy are given in Table 1.

3.3 CTS Test

Mixed mode fracture response of neat epoxy was investigated using the compact tension shear (CTS) test. The test setting included a CTS specimen inside a CTS fixture (see Fig. 1(a) and (b)). The geometry of the CTS specimen is shown in Fig. 1(c) and (d). The mode of loading was changed from $\alpha = 0^{\circ}$ (pure mode I, Fig. 1(a)) to $\alpha = 90^{\circ}$ (pure mode II, Fig. 1(b)) in the specimen by changing the location of the pin. Total length of the notch, a, was half of the specimen width [13]. A pre-crack of

0.5mm long was cut by a razor blade at the notch tip. The temperature effects due to the frictional heating by the blade should be avoided, and for this reason, each specimen was tested at least one day after they were cut by the blade.

The load was applied by an Instron servohydraulic load frame (Instron 8804) and it was measured by a 250kN or a 5kN load cell, depending on the expected value of the maximum load. The displacement rate was 2mm/min and the displacement was measured at the cross head of the testing machine. The test was performed at room temperature with 50% relative humidity.

The maximum load from which the crack opens, was measured during the test. This value was used to calculate mode I and mode II critical stress intensity factor (SIF) of epoxy, K_{Ic}, and K_{IIc} respectively.

3.4 SENB Test

Single edge notch beam (SENB) tests were also performed to determine the value of pure mode I CSERR [15]. The SENB testing was performed in accordance with ASTM 5045 [16], and was carried out on rectangular neat epoxy specimens with a length of 130 mm, a width of 28 mm and a thickness of 14 mm . A tiny slit with a length of 14mm was cut in the middle of the specimen and a 0.5 mm long crack was made by a cutting blade at the tip of the slit (See Fig. 1(e)).

Fracture surfaces of CTS and SENB specimens were extracted for subsequent imaging by a scanning electron microscopy (SEM) or stereomicroscopy by cutting carefully at a low rate and keeping them away from humidity to decrease the post-failure damage on the fracture surface [17].

3.5 CTS specimen modifications

For higher mode II loads, epoxy specimens failed at the bolt hole before the beginning of the crack propagation at the notch tip. In order to solve the problem and perform valid tests, composite tabs with a length of 60 *mm* and width of 38 *mm*, made of woven glass epoxy were used to resist to the bolt hole stress concentration. The composite tabs were glued to the epoxy specimen and cured at room temperature during 48 hours to avoid post curing effect on the epoxy specimen. The bolt holes were

then made by drilling the tabbed specimens. Finally, this modification on CTS specimens allow a failure at the notch tip [18].

4. Failure model

A notched polymer specimen as shown in Fig. 2 was firstly considered. A nominal stress of σ at an arbitrary angle α was applied to the CTS specimen. The stress applied to the specimen was assumed to resolve into shear and normal components (i.e. σ_y and τ_{xy}) according to the following relations:

$$\sigma_y = \sigma\cos\alpha \quad (1)$$

$$\tau_{xy} = \sigma\sin\alpha \quad (2)$$

where $\sigma = \frac{F}{width \times thk.}$. The values of the mode I and mode II stress intensity factors denoted K_I and K_{II} respectively, at the specimen crack tip can be obtained with the following expansion [19]:

$$K_I = Y_1\sigma_y\sqrt{\pi a} \quad (3)$$

$$K_{II} = Y_2\tau_{xy}\sqrt{\pi a} \quad (4)$$

Dimensionless geometric components, Y_1 and Y_2 which will be introduced later, depend on the specimen width, *w*, and the crack length, *a*. Substituting shear and normal stress components of Equations 1 and 2 into Equations 3 and 4 the expansion of SIF can be written as:

$$K_I = Y_1\,\sigma\cos\alpha\,\sqrt{\pi a} \quad (5)$$

$$K_{II} = Y_2\,\sigma\sin\alpha\,\sqrt{\pi a} \quad (6)$$

Defining the effective value of stress intensity factor, $K_{eff.}$, as:

$$K_{eff.} = \sqrt{K_I^2 + K_{II}^2} \quad (7)$$

Assuming a plane strain condition, the material CSERR can then be obtained:

$$G_c = K_{eff}^2\frac{1-v^2}{E} = \frac{(K_I^2 + K_{II}^2)(1-v^2)}{E} \quad (8)$$

Substituting the values of K_I and K_{II} from Equations 5 and 6 into Equation 8, an expression for the CSERR as a function of a loading angle can be given:

$$G_c = \cos^2\alpha \frac{\mathrm{K_{Ic}^2}(1-\nu^2)}{\mathrm{E}} + \sin^2\alpha \frac{K_{IIc}^2(1-\nu^2)}{E} \quad (9)$$

Since:

$$G_{Ic} = \frac{\mathrm{K_{Ic}^2}(1-\nu^2)}{\mathrm{E}} \quad (10)$$

$$G_{IIc} = \frac{\mathrm{K_{IIc}^2}(1-\nu^2)}{\mathrm{E}} \quad (11)$$

Therefore, Equation 9 can be rewritten as:

$$G_c = \cos^2\alpha\ G_{Ic} + \sin^2\alpha\ G_{IIc} \quad (12)$$

Equation 12 predicts an "S-curve" behaviour between G_{Ic} and G_{IIc} for the mixed mode toughness versus loading angle. Richard [20], using the finite element method, developed the following expressions for Y_1 and Y_2:

$$Y_1 = \frac{1}{1-\frac{a}{w}}\sqrt{\frac{0.26+2.65\left(\frac{a}{w-a}\right)}{1+0.55\left(\frac{a}{w-a}\right)-0.08\left(\frac{a}{w-a}\right)^2}} \quad (13)$$

$$Y_2 = \frac{1}{1-\frac{a}{w}}\sqrt{\frac{-0.23+1.4\left(\frac{a}{w-a}\right)}{1-0.67\left(\frac{a}{w-a}\right)+2.08\left(\frac{a}{w-a}\right)^2}} \quad (14)$$

K_I and K_{II} are calculated using the following expanded equations [20]:

$$K_I = \frac{P\sqrt{\pi a}}{wt} \times \frac{cos\alpha}{1-\frac{a}{w}}\sqrt{\frac{0.26+2.65\left(\frac{a}{w-a}\right)}{1+0.55\left(\frac{a}{w-a}\right)-0.08\left(\frac{a}{w-a}\right)^2}} \quad (15)$$

$$K_{II} = \frac{P\sqrt{\pi a}}{wt} \times \frac{sin\alpha}{1-\frac{a}{w}}\sqrt{\frac{-0.23+1.4\left(\frac{a}{w-a}\right)}{1-0.67\left(\frac{a}{w-a}\right)+2.08\left(\frac{a}{w-a}\right)^2}} \quad (16)$$

where *t* , *w* and *a* are the specimen thickness, width and crack length respectively. Using the critical (maximum) load that opens the crack, P_{max} , the critical stress intensity factor (K_{Ic} *and* K_{IIc}) of the material can be calculated.

5. Results and Discussion

4.1 Plane strain condition

The determination of K_{Ic}requires that a plane strain condition exists at the crack tip [19]. Therefore, the effect of thickness of the epoxy specimens on the value of fracture toughness was studied. For this purpose different thicknesses from 2 *mm* to 13.5 *mm* were used. CTS specimens with thicknesses ranging from 2 *mm* to 7.5 *mm* and SENB specimens from 12 *mm* to 13.5 *mm* were tested. The results for pure mode I fracture toughness and CSERR are shown in Fig. 3(a) and b respectively. As can be seen in Fig. 3(a) and (b), a minimum thickness of 7.5 *mm* is required for the epoxy specimen to ensure a state of plane strain that gives correct value for K_{Ic}. It is recommended (e.g. [19]) that the ratio of the plastic radius, r_p, at the tip of the crack to the thickness of the material t (i.e. $\frac{r_p}{t}$) should be of order of 0.025 to ensure having plain strain condition in the material. The size of the plastic radius was calculated by $r_p = \frac{K_{Ic}^2}{6\pi\sigma_y^2}$ in which σ_y is the yield stress of the material. The relation predicts a plastic radius of 200 micrometers for epoxy and so, the approximate minimum thickness of epoxy should be equal to 8 *mm*, which is consistent with the value of 7.5 mm measured experimentally. Here, as the size of plastic zone ahead of the crack tip is negligible compared to other dimensions of the specimen, Linear Elastic Fracture Mechanics (LEFM) can be used in the relations.

The results show average values of 3.07 $MPa\sqrt{m}$ and 2.85 $\frac{kJ}{m^2}$ for pure mode I fracture toughness and pure mode I CSERR respectively. As discussed in the failure model, to calculate the values of CSERR mechanical properties (E and ν) of epoxy is required. These properties were measured using tensile testing and are summarized in Table 1.

5.2 Mixed mode fracture response

The values of the mode II fracture toughness and the CSERR for specimens having minimum thickness of 7.5 mm were measured using CTS specimen and are equal to $K_{IIc} = 4.89\ MPa\sqrt{m}$ and $G_{IIc} = 7.05\frac{kJ}{m^2}$ respectively.

As shown in Fig. 4, the value of maximum load increases from 2200N for pure mode I ($\alpha = 0^{\circ}$) to 3200N for pure mode II ($\alpha = 90^{\circ}$), which results in higher value of fracture toughness and CSERR. The values of mode I and mode II components of the fracture toughness can be calculated from Equations 15 and 16. These values are used to determine the effective fracture toughness which is the root mean square of mode I and mode II components of fracture toughness as shown in Fig. 5. Fig. 6(a) shows the value of CSERR (G_c) vs. different modes of loading for neat epoxy. In total 19 specimens were tested: i.e. 5 in pure mode I and pure mode II, 3 under 75 degree, 2 specimens at each angle of 15° and 30° and 1 specimen at angle of 45° and 60°.

As it can be seen in Fig. 6(a), CSERR in mode II is almost 2.47 times greater than the value of CSERR for the mode I, which is in agreement with Bruce [12] and experiments carried out by Araki etal. [11]. The increase in the value of mode II CSERR is related to the size of the plastic radius in front of the crack and the morphology of the fracture surface that will be discussed in Section 5.4.

5.3 Crack Growth Angle

The crack growth angle is the angle from which the crack opens up under different loading modes. The prediction of the crack path was firstly studied by Erdogan and Sih [21] who used the maximum principal stress criterion and Sih [22] who employed the minimum strain energy density criterion. The value of the crack growth angle in CTS specimen was predicted using an empirical relation introduced by Richard etal. [23]:

$$\varphi_0 = \pm\left[155.5^{\circ}\frac{|K_{II}|}{|K_I| + |K_{II}|}\right] - 83.4^{\circ}\left[\frac{|K_{II}|}{|K_I| + |K_{II}|}\right]^2 \qquad (17)$$

where K_I and K_{II} are mode I and mode II components of fracture toughness respectively. Epoxy specimens under mode I loading begin to fracture at the notch tip, as the crack propagates in a path parallel to the notch direction. The propagation angle varies from 0° to 85°. The comparison between

the predicted value and the measured value exhibits a good agreement (with maximum deviation of %9.5) as shown in Fig. 6(b).

5.4 Fractography

In this section, the influence of parameters such as thickness and loading modes on the fracture morphology is discussed.

5.4.1 Effect of specimen thickness on fracture morphology

It was shown that thicker specimens result in a lower value of fracture toughness and CSERR (Fig. 3(a) and (b)) as a result of the transition from plane strain (thick specimens) to plane stress in thinner specimens. A flat fracture area is observed for thicker specimens subjected to loading angles close to 0° whereas a fracture surface with evidence of plastic deformation, hackles and chevron patterns is observed for thinner specimens (Fig. 7(a) and (b): pure mode I loading, Fig. 7(c) and (d): 15° loading angle). It is obvious that a flat fracture surface requires smaller amount of energy to propagate, which results in a smaller value of toughness in thicker specimens.

5.4.2 Effects of the Mode of Loading

Observations of the fracture surface reveal that the morphology is changing as the loading changes from pure mode I to pure mode II. The fracture surface of the specimen under pure mode I shows a neat cleavage fracture surface, as shown in Fig. 8(a). A flat surface is caused by the tensile stresses acting normal to the surface. A flat fracture surface releases a smaller amount of energy during the fracture compared to the other type of fracture areas. Increasing the loading angle from 0° towards 90°, the resulting fracture morphology is no longer flat. SEM and stereomicroscopy images show radial patterns on the fracture surface, which are observed in lower angles of loading and indicate sharp and fast crack propagation. This pattern can be observed on the fracture surface of specimens subjected to 15° loading angle for instance (see Fig. 8 b). For higher degrees of mode II, chevron and river patterns

are observed on the surface (Fig. 8(c) and (d)). These morphologies reveal extensive resin plastic deformation and extension that require a higher value of energy to propagate.

Fig. 9 shows the comparison of the criterion prediction (Equation 12) and the experimental values of mixed mode CSERR with standard deviation. The expected "*S"* pattern is observed for the values of mixed-mode CSERR and the predictions based on Equation 12 fit well with experimental results. A similar "*S"* pattern is also observed in the mixed mode fracture of adhesives [3].

5.4.3 Hackles

Hackles or cusps (Fig. 8(d)) are the dominant fractographic feature for higher mode II [17]. Hackles appear inclined opposite to the direction of the crack propagation. Thus, they can be used to determine how crack has been locally propagated. The size of the hackles has been shown to depend on moisture content, temperature and matrix toughness [17,24]. For instance, higher temperature increases the plasticity leading to thicker hackles and increased CSERR of the material. The formation of hackles in polymers during fracture has been discussed by Purslow [25]. According to him, if there is shear loading in the area close to the crack tip due to the mode II loading, it can be resolved into principal stress. Principal stress is a tensile stress on the region in front of the crack. The pure mode II principal stress acts in 45° angle with regard to the crack direction. This tensile stress develops a crack in the polymer in 45° angle and hackles appear by connection of these cracks.

The geometry of hackle requires larger area absorbing energy compared to a flat surface in mode I loading, which was confirmed in our test results.

For thinner specimens subjected to mode II, macro hackles were observed. In Fig. 10, multiple hackles started from a few millimeters away from the crack tip and result in higher value of mode II CSERR (about 12 $\frac{\mathrm{KJ}}{\mathrm{m}^2}$) for epoxy.

6. Conclusions

The fracture and tensile behaviour of an epoxy was characterized using dumbbell shape specimens and a combination of compact tension shear and single edge notched beam specimens. To ensure fracture

at the tip of the crack under pure mode II, specimens were modified by composite tabs. The mode I and mode II critical strain energy release rates were determined to be 2.85 $\frac{KJ}{m^2}$ and 7.05 $\frac{KJ}{m^2}$ respectively. The ratio $\frac{G_{II}}{G_I} = 2.47$ is in agreement with the model proposed by Bruce [12] based on the increased surface area resulting from hackle formation in mode II fracture. It suggests that that mode II and mixed mode fracture properties of a material can be predicted if the mode I properties are known. The mixed mode CSERR was well predicted by a micromechanical model that accounts for the transition of resolved normal and shear components of the mixed mode loading acting on the crack. Fracture morphology and its relation to the value of toughness of the epoxy subjected to different modes of loading were observed and investigated. The effect of thickness on the fracture morphology was also investigated. The increase in the toughness for the mode II loading was related to the hackles formation on the fracture surface of the resin.

Based on our study, the next piece of work is to look at the effect of constraint on the energy absorbed by the bond (resin) during the mixed mode fracture to predict the contribution of adhesive toughness to the total toughness of composite material. When a bulk adhesive such as bulk epoxy fractures a major portion of energy dissipates in the material due to its plastic deformation before fracture. The amount of plastic deformation is however limited in a fibrous polymer composite by the neighboring fibres or in a bond by the neighboring adherends. This difference results in a higher value of toughness in bulk epoxy compared to a reinforced epoxy. As a result in this case the value of epoxy toughness should be scaled by the ratio of the reinforced material that is being plastically deformed. The result can be used to calculate the reinforced resin toughness based on the toughness of bulk resin towards predicting the fracture behavior of a polymer composite or bond.

7. Acknowledgments

The first author would like to acknowledge Dr. Tom Bruce and Dr. Abdel-Hamid Mourad for their helpful comments. Funding for this research was provided by the International Composites Research Center which was established as a result of a grant from the Ontario Research Foundation.

References:

[1] Reeder JR. An Evaluation of Mixed-Mode Delamination Failure Criteria. NASA Tech Memo 104210 1992:1–57.

[2] Hahn H. A mixed-mode fracture criterion for composite materials. Compos Technol Rev 1983;5:26–9.

[3] Ducept F, Davies P, Gamby D. Mixed mode failure criteria for a glass/epoxy composite and an adhesively bonded composite/composite joint. Int J Adhes Adhes 2000;20:233–44. doi:10.1016/S0143-7496(99)00048-2.

[4] Balzani C, Wagner W, Wilckens D, Degenhardt R, Büsing S, Reimerdes HG. Adhesive joints in composite laminates - A combined numerical/experimental estimate of critical energy release rates. Int J Adhes Adhes 2012;32:23–38. doi:10.1016/j.ijadhadh.2011.09.002.

[5] Ashcroft I a., Hughes DJ, Shaw SJ. Mode I fracture of epoxy bonded composite joints: 1. Quasi-static loading. Int J Adhes Adhes 2001;21:87–99. doi:10.1016/S0143-7496(00)00038-5.

[6] Wu S, Guo Q, Peng S, Hameed N, Kraska M, Mai Y. Nanostructure − Mechanical Property Correlation. Macromolecules 2012;45:3829–40.

[7] Pearson R a., Blackman BRK, Campilho RDSG, De Moura MFSF, Dourado NMM, Adams RD, et al. Quasi-Static Fracture Tests. Test Adhes Joints, Best Pract 2012:163–271. doi:10.1002/9783527647026.ch3.

[8] Chen Z, Adams RD, Da Silva FM. Fracture toughness of bulk adhesives in mode I and mode III and curing effect. Int J Adhes Adhes 2011;167:221–34. doi:10.1007/s10704-010-9547-9.

[9] Maccagno T, Knott J. The fracture behaviour of PMMA in mixed modes I and II. Eng Fract Mech 1989;34:65–86.

[10] Chen Z, Adams RD, Da Silva FM. The use of the J -integral vector to analyse adhesive bonds with and without a crack. Int J Adhes Adhes 2011;31.1:48–55. doi:10.1016/j.ijadhadh.2010.11.005.

[11] Araki W, Nemoto K, Adachi T, Yamaji A. Fracture toughness for mixed mode I/II of epoxy resin. Acta Mater 2005;53:869–75. doi:10.1016/j.actamat.2004.10.035.

[12] Bruce TP. Mechanistic Mixed-Mode Failure Criterion For Continuous Fiber-Polymer Composites. PhD thesis, Mechanical and Materials Engineering Department Western University, Canada. 2011.

[13] Richard HA, K . Benitz. A loading device for the creation of mixed mode in fracture mechanics. Int J Fract 1983;22:55–8.

[14] ASTM D638-10. Standard Test Method for Tensile Properties of Plastics. ASTM 2010:1–16. doi:10.1520/D0638-10.1.

[15] Jamali J, Wood JT. Mixed-mode through-thickness fracture of polymer matrix composites. 19th Int. Conf. Compos. Mater. (ICCM 19), Montr. Canada, Montreal, Canada: 2013, p. 6453–62.

[16] ASTM D5045. Standard Test Methods for Plane-Strain Fracture Toughness and Strain Energy Release Rate of Plastic Materials 1999;99. doi:10.1520/D5045-99R07E01.2.

[17] Greenhalgh E. Failure analysis and fractography of polymer composites. vol. 10. CRC press; 2009.

[18] Jamali J. Mechanistic Failure Criterion for Unidirectional and Random Fibre Polymer Composites. PhD thesis, Mechanical and Materials Engineering department, The University of Western Ontario, London, Ontario, Canada, 2014.

[19] Broek D. Elementary engineering fracture mechanics. 2nd ed. Hingham, MA, USA: Springer; 1982.

[20] H. Richard. Some theoretical and experimental aspects of mixed mode fractures. Adv Fract Res 1984:3337–44.

[21] Erdogan F, Sih G. On the crack extension in plates under plane loading and transverse shear. J Basic Eng 1963;85:519–25.

[22] Sih G. Strain-energy-density factor applied to mixed mode crack problems. Int J Fract 1974;10:305–21.

[23] Richard H a., Fulland M, Sander M. Theoretical crack path prediction. Int J Fract 2005;28:3–12. doi:10.1111/j.1460-2695.2004.00855.x.

[24] Gude MR, Prolongo SG, Ureña a. Hygrothermal ageing of adhesive joints with nanoreinforced adhesives and different surface treatments of carbon fibre/epoxy substrates. Int J Adhes Adhes 2013;40:179–87. doi:10.1016/j.ijadhadh.2012.09.005.

[25] Purslow D. Matrix fractography of fibre-reinforced epoxy composites. Composites 1986;17:289–303. doi:10.1016/0010-4361(86)90746-9.

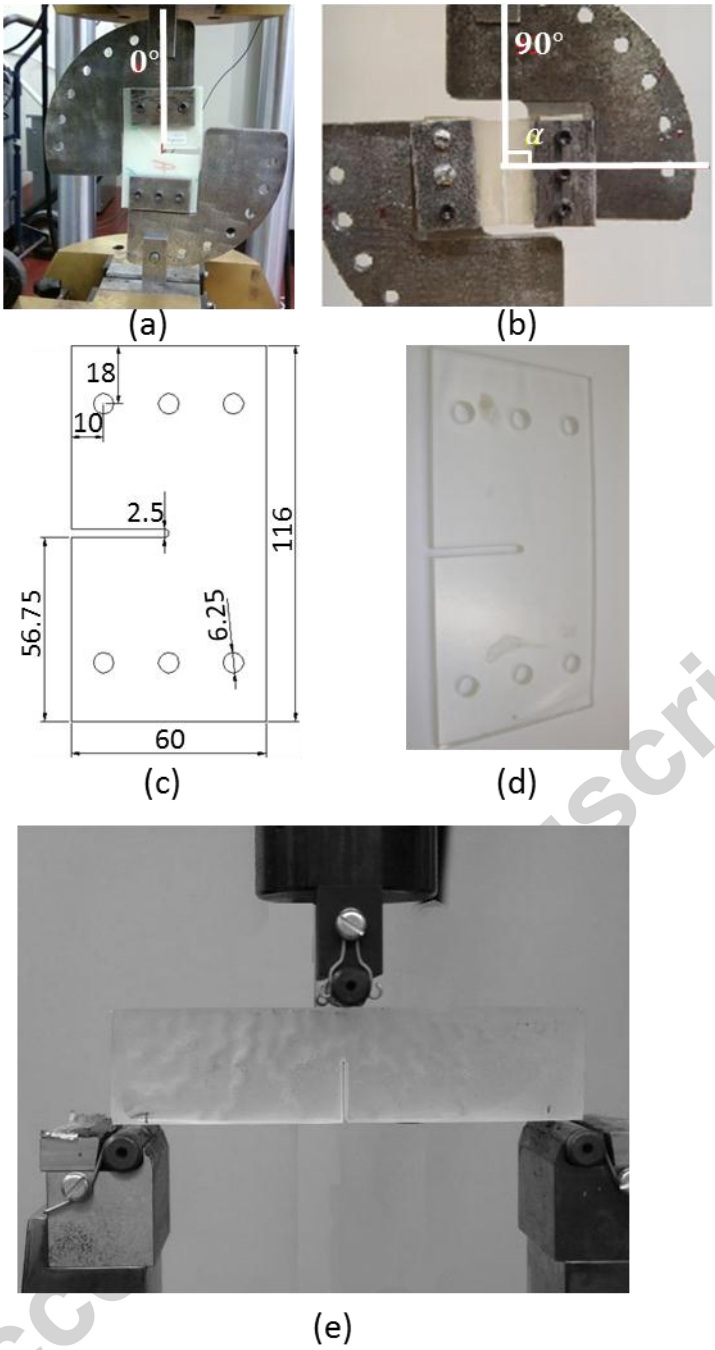

Fig. 1 CTS fixture. (a) pure mode I. (b) pure mode II loading. CTS specimen (c) 2D drawing (d) neat epoxy specimen after machining. (e) Single edge notch beam lab setting.

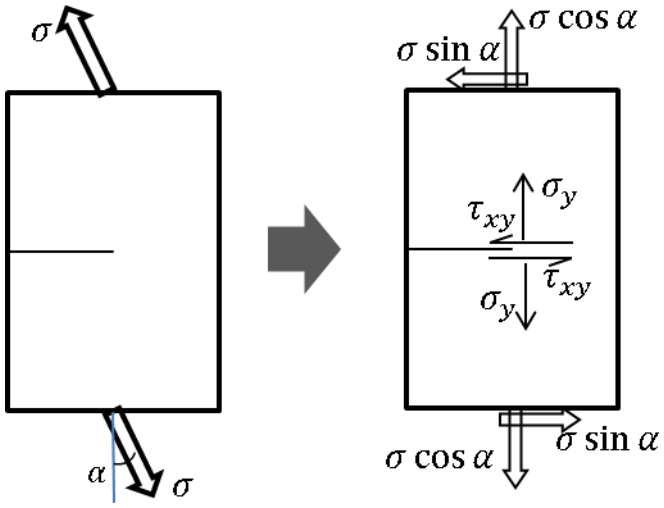

Fig. 2 General state of stress at the elements shown in the CTS sample for a mixed mode I and II and crack propagation under mixed mode loading.

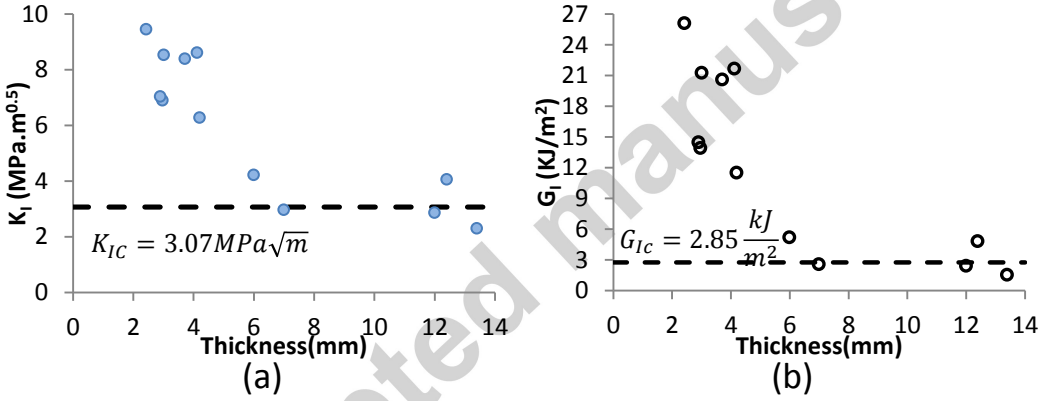

Fig. 3 Thickness effect on (a) mode I fracture toughness and (b) mode I toughness.

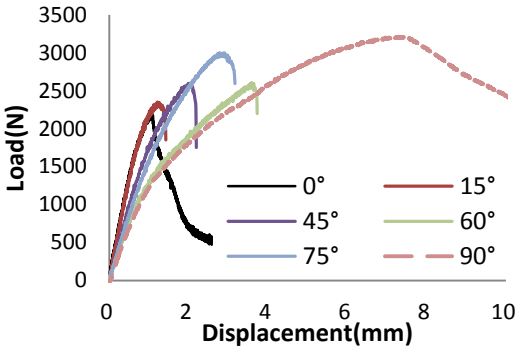

Fig. 4 Epoxy load-displacement, sample thicknesses between 3 and 4mm.

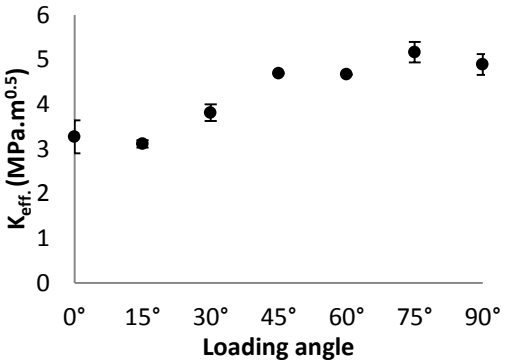

Fig. 5 Effective fracture toughness vs. loading angle.

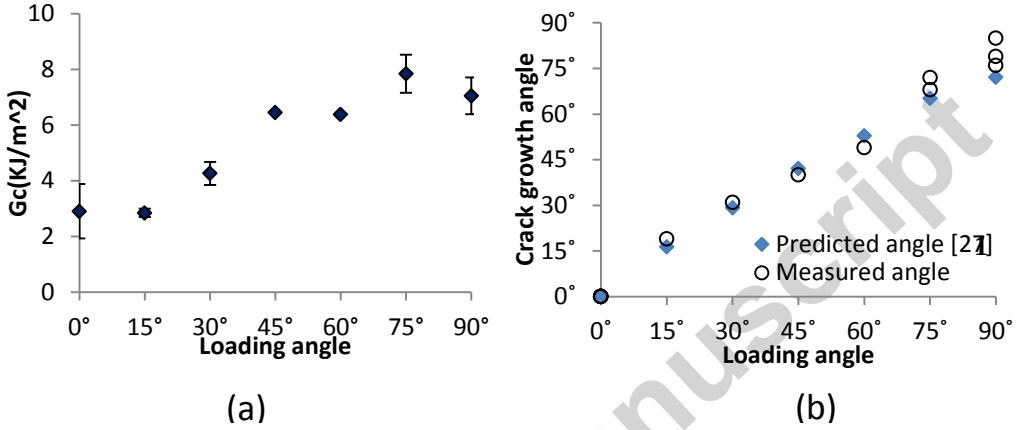

Fig. 6 (a) Mixed mode toughness vs. loading angle. (b) Comparison of measured and predicted values of crack growth angle.

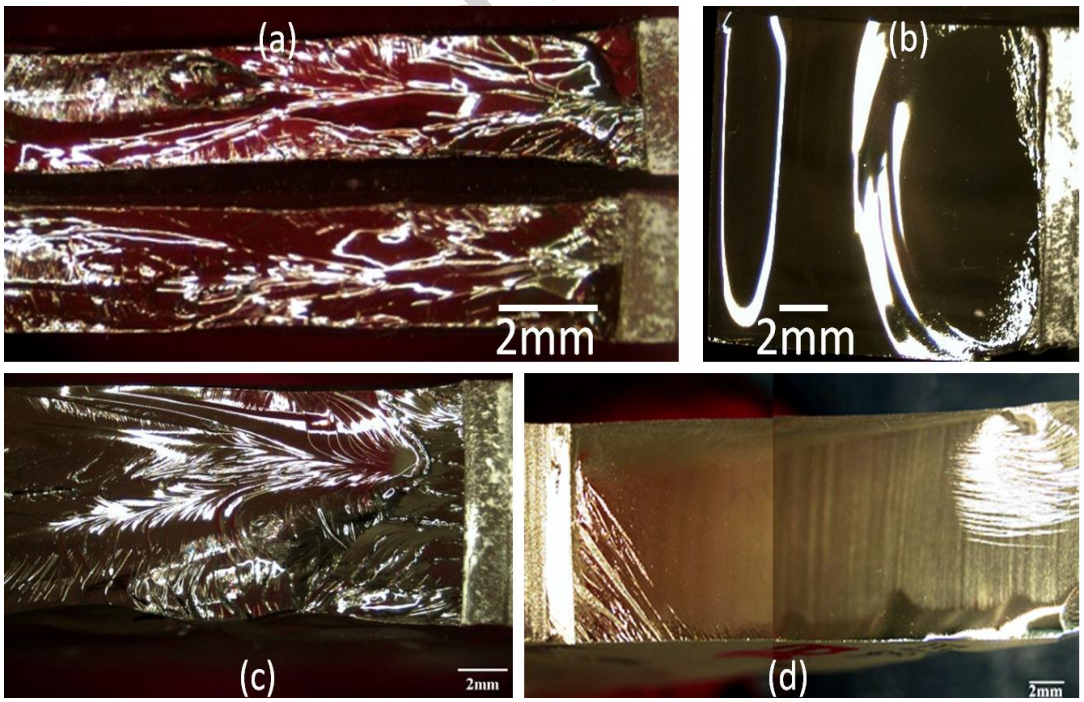

Fig. 7 Comparison of epoxy specimen's fracture surface morphologies. Specimens were subjected to (a) mode I (loading angle of 0°) with thickness of 3 mm and (b) thickness of 12 mm, (c) loading angle of 15° with thickness of 6.8 mm and (d) thickness of 12 mm.

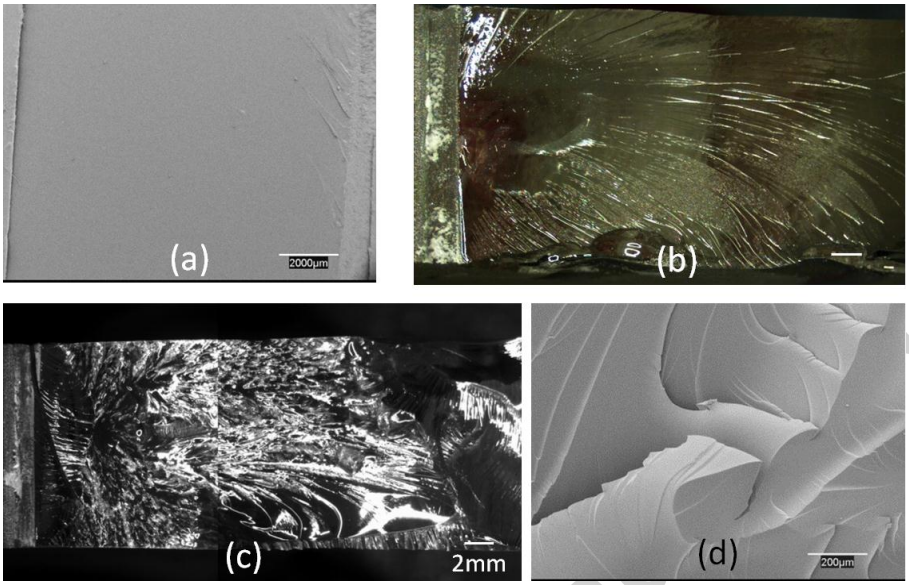

Fig. 8 SEM and steromicroscopy image of the fracture surface of epoxy under (a) pure mode I testing (b) 15° of loading angle (c) 75° of loading angle and (d) pure mode II testing with hackles.

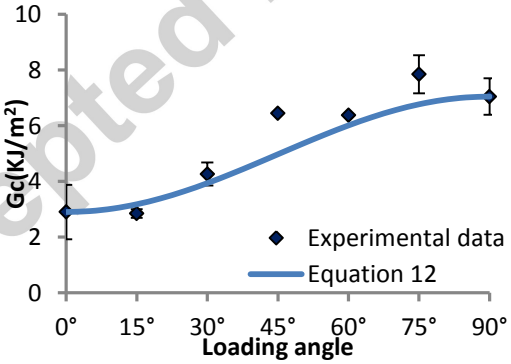

Fig. 9 Comparison of CSERR predicted for epoxy by failure criterion (Equation 12) and experimental data.

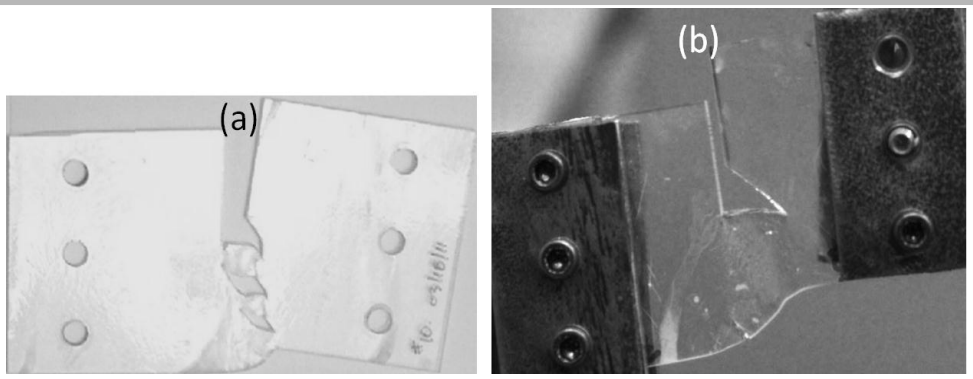

Fig. 10 Macro hackles in some of neat epoxy specimen under mode II loading, sample with macro hackle (a) sample without macro hackling (b).

Mechanical Properties		Unit
E	2.9±0.15	GPa
σ_y	30.8±5	MPa
υ_{12}	0.38*	-
ε_f	4.1±0.91	%
ρ	1.18	$\frac{\text{gr}}{\text{cm}^3}$
σ_{ut}	61±0.88	MPa

Table 1 Mechanical properties of epoxy (CLR1180/CLH6560 Crosslink) used in the calculations.

*Poisson's ratio is taken from Cambridge Engineering Selector (CES) EduPack.